

Degradation and damage behaviors of steel frame welded connections

Meng Wang^{*1}, Yongjiu Shi^{2a}, Yuanqing Wang^{2b}, Jun Xiong² and Hong Chen³

¹ School of Civil Engineering, Beijing Jiaotong University, Beijing 100044, China

² Department of Civil Engineering, Tsinghua University, Beijing 100084, China

³ Architectural Design and Research Institute, Tsinghua University, Beijing 100084, China

(Received December 13, 2011, Revised June 10, 2013, Accepted July 22, 2013)

Abstract. In order to study the degradation and damage behaviors of steel frame welded connections, two series of tests in references with different connection constructions were carried out subjected to various cyclic loading patterns. Hysteretic curves, degradation and damage behaviours and fatigue properties of specimens were firstly studied. Typical failure modes and probable damage reasons were discussed. Then, various damage index models with variables of dissipative energy, cumulative displacement and combined energy and displacement were summarized and applied for all experimental specimens. The damage developing curves of ten damage index models for each connection were obtained. Finally, the predicted and evaluated capacities of damage index models were compared in order to describe the degraded performance and failure modes. The characteristics of each damage index model were discussed in depth, and then their distributive laws were summarized. The tests and analysis results showed that the loading histories significantly affected the distributive shapes of damage index models. Different models had their own ranges of application. The selected parameters of damage index models had great effect on the developing trends of damage curves. The model with only displacement variable was recommended because of a more simple form and no integral calculation, which was easier to be formulated and embedded in application programs.

Keywords: welded connection of steel frame; degradation and damage behaviours; low-cycle fatigue; damage index model; failure mode

1. Introduction

Damage or collapse of steel structure subjected to extreme earthquake is a complex phenomenon, generally caused by buckling and fracture of members and connections. All these behaviors are accompanied with large cumulative plastic deformation under cyclic loading patterns, leading to degradation of capacity and stiffness. This process can be equivalently described as extremely low cycle fatigue with large inelastic strains (National Natural Science Foundation Committee 2006, Lignos 2008, Zareian 2006).

Actually, these seismic responses may cause complex failure modes (Wang *et al.* 2009,

*Corresponding author, Ph.D., E-mail: wangmeng1117@gmail.com

^a Professor Ph.D. E-mail: shiyj@mail.tsinghua.edu.cn

^b Professor Ph.D. E-mail: wang-yq@mail.tsinghua.edu.cn

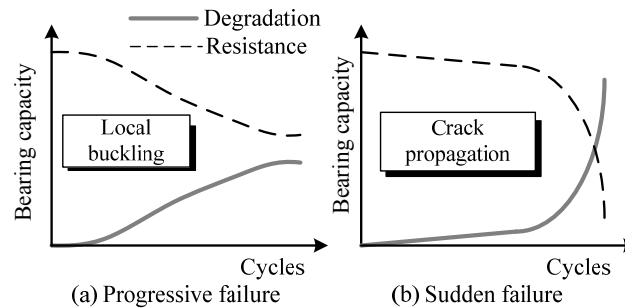


Fig. 1 Distributive curves of damage index models

Papagiannopoulos and Beskos 2011). Based on the degraded behaviors of connections, the collapse or failure is classified into three modes, progressive failure, sudden failure, and mixed failure (Krawinkler and Zohrei 1983, Castiglioni *et al.* 2007, Castiglioni and Pucinotti 2009). 1) In the case of Fig. 1(a), the progressive failure mode shows an obvious and gradual degradation of strength and stiffness caused by formation of a plastic hinge. This failure is related to local buckling of beam flange and web subjected to cyclic loading, and a gradually propagative crack initiates at steel plate when the strain reaches the ultimate tensile strain of steel material. 2) As shown in Fig. 1(b), sudden failure occurs suddenly without any signs, accompanying with the propagation of cracks at either welded toe or heat affected zone. The specimens do not show noticeable decrease of strength and stiffness with increasing of cycles before being completely destroyed. However, once degradation occurs, the members suffer failure in few cycles. 3) Mixed failure mode appears between two previous failure modes. Initially, degraded phenomena are not obvious. But later the failure is finally associated with local buckling of plates and crack propagation along welded toes or base metal.

Based on the probable failure modes, accurate evaluation of cumulative damage effect on structures and actual prediction for failure modes are necessary for estimating the remainder life of structures (Ballio *et al.* 1997, Li 2002, Li *et al.* 2004). The damage process may cause the redistribution of internal forces in members, affecting the final failure modes. In order to assess the reliability of structures subjected to severe earthquakes, a method was proposed by defining damage index. This method is convenient to predict the damage degrees and probable failure of structures under cyclic loadings. Many studies have proposed various damage index models. Some of them (or their criteria) were suitable for steel structures and most of them were proposed for reinforcement concrete members. Whether these models can give the actual predicted results should be answered and their applicability for steel frame structures should be studied and discussed.

The purpose of this study is to analyze degradation and damage behaviors of welded connections of steel frames. Two series of quasi static tests including total nineteen specimens were adopted, which were carried out by Tsinghua University. In these tests, different constructions and different cyclic loading patterns were designed to investigate their effects on seismic behaviors and failure modes. Hysteretic curves, degradation and damage behaviours and fatigue properties were discussed, and then typical failure modes and probable reasons were also analyzed. According to the experimental results, the dissipative energy, cumulative dissipative energy, imposed displacement, imposed force, yield displacement and yield force of each

connection in per cycle were calculated respectively. In terms of these basic data, distributive curves of ten damage index models for each connection were obtained. And then, predicted capacities of these models for degraded properties and failure modes were analyzed and compared. Furthermore, the accuracy of collapse prediction was verified by the selected models. The differences of damage index models with different controlling factors were also discussed.

2. Beam-to-column experimental programs

In order to investigate the influencing factors of degradation behaviors and failure modes, two series of beam-to-column tests were carried out in Tsinghua University (Chen 2001, Xiong 2011). The first series focused on various connection constructions to improve failure modes. The second series further studied the effect of loading histories and loading amplitudes on degraded characteristics and final damage modes. These two series of tests were analyzed and discussed in details below respectively.

2.1 Chen (2001) tests from Tsinghua University

2.1.1 Specimens description

In order to study the seismic behaviors of improved welded beam-to-column connections, a group of sixteen specimens were tested subjected to various cyclic loading patterns. Ten specimens with typical failure modes were adopted for analysis. The connected method of beam and column was that beam flanges were welded to column flange and beam web was bolted to the shear tab, which was recommended by “Code for seismic design of buildings (GB 50011-2001)” in China. The detailed dimensions of connection specimen were shown in Fig. 2, consisting of a welded beam section H-400 × 150 × 8 × 12 (mm) and a welded column section H-450 × 250 × 12 × 16 (mm) based on the principle of “strong column and weak beam.” These sections satisfied the requirements of Chinese national standard (GB 50011-2001). L_B (the length of beam) was 1800 mm. Four connected bolts (diameter is 20 mm) were frictional high strength bolts, whose yield

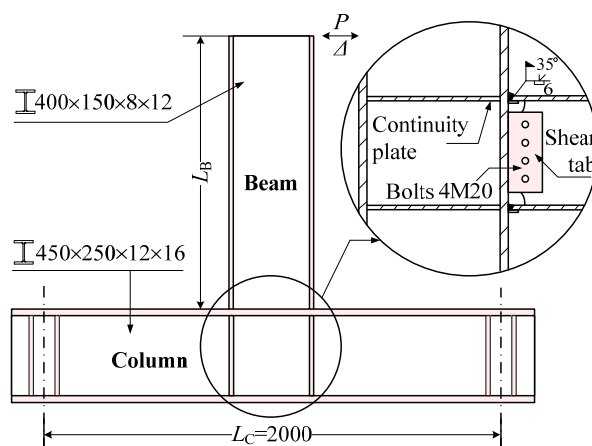


Fig. 2 Experimental setup

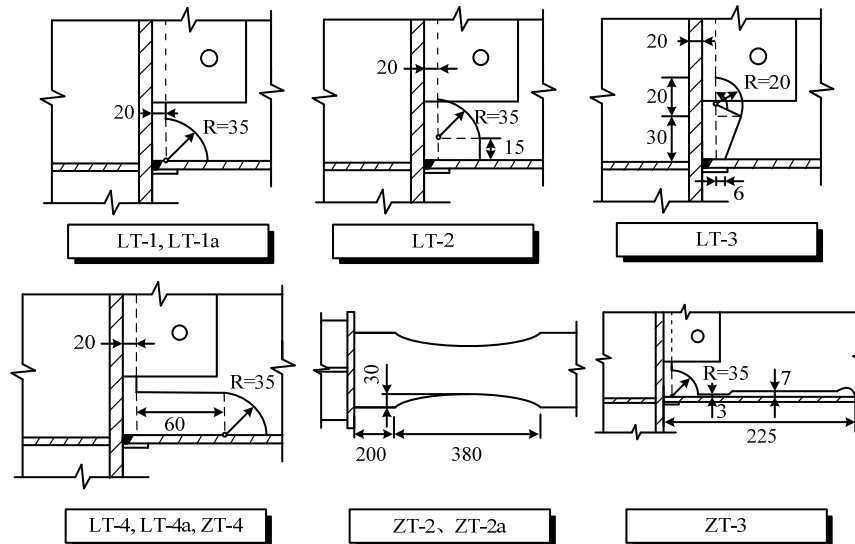


Fig. 3 Specimen constructions (mm)



Fig. 4 Experimental setup

strength were 1090 MPa.

In order to change the failure modes of structures, several connection constructions were designed, including standard connections (LT-1 and LT-1a), enlarged access hole connections (LT-2, LT-3, LT-4, LT-4a and ZT-4), “dog bone” connections (ZT-2 and ZT-2a) and elongated slot in web connection (ZT-3). “Dog bone” specimens and specimen with elongated slot in web were designed according to Reference (Egor *et al.* 1998). The dimensions of the constructions were shown in Fig. 3. The specimens described in this paper were fabricated from Q235B steel and yield strength of steel material was 270 MPa as reported.

The cyclic loadings were imposed on the specimens using a servo control jack machine of ± 5000 kN capacity as shown in Fig. 4. The values of reaction force, imposed displacement and strain were obtained from IMP data equipments. All the specimens were force-displacement controlled and the loading patterns were summarized in Fig. 5 and Table 1, with both constant amplitude loading and stepwise amplitude loading.

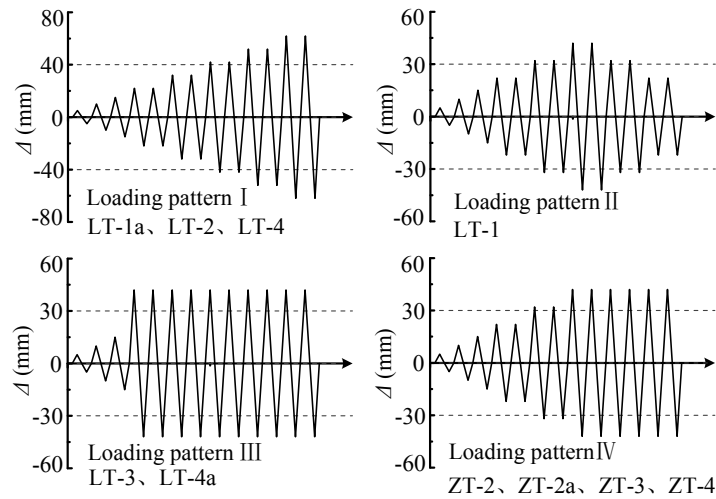


Fig. 5 Cyclic loading patterns

Table 1 Failure parameters of specimens

Details	Spec.	N_{total}	N_p	Loading patterns	Failure modes
Typical	LT-1	13	11	II	△
	LT-1a	9	7	I	○
Dog bone	ZT-2	10	8	IV	○
	ZT-2a	8	6	IV	○
Elongated slot	ZT-3	12	10	IV	□
Access hole I	LT-2	9	7	I	○
Access hole II	LT-3	4	4	III	□
Access hole III	LT-4	8	6	IV	△
	LT-4a	10	10	III	□
	ZT-4	12	10	I	○

*Note: □ Progressive failure mode, △ Mixed failure mode, ○ Sudden failure mode

2.1.2 Results and discussion

Hysteretic curves ($P-\Delta$) of specimens were shown in Fig. 6. The typical failure modes of the connections were also presented in Fig. 6. From the observations in tests, most of connections fractured at the heat affected zones of beam bottom flange welds, leading to brittle failures. The probable reasons were that the mechanical properties of heat affected zone and base metal were non-uniformity, causing stress concentrations at the interface. Besides, the ductility of weld was worse than base metal under cyclic loading. Specimen ZT-3 suffered fatigue damage at weld of bottom flange, because of weak interactive restraints of web and flange. Specimen LT-4a presented obvious local buckling phenomenon near the enlarged weld access hole (shown in Fig. 6). From the hysteretic curves and failure modes, the damage developing processes were obviously classified into progressive failure, sudden failure, and mixed failure. Table 1 summarized the types of failure, total number of cycles, number of plastic cycles, and loading histories.

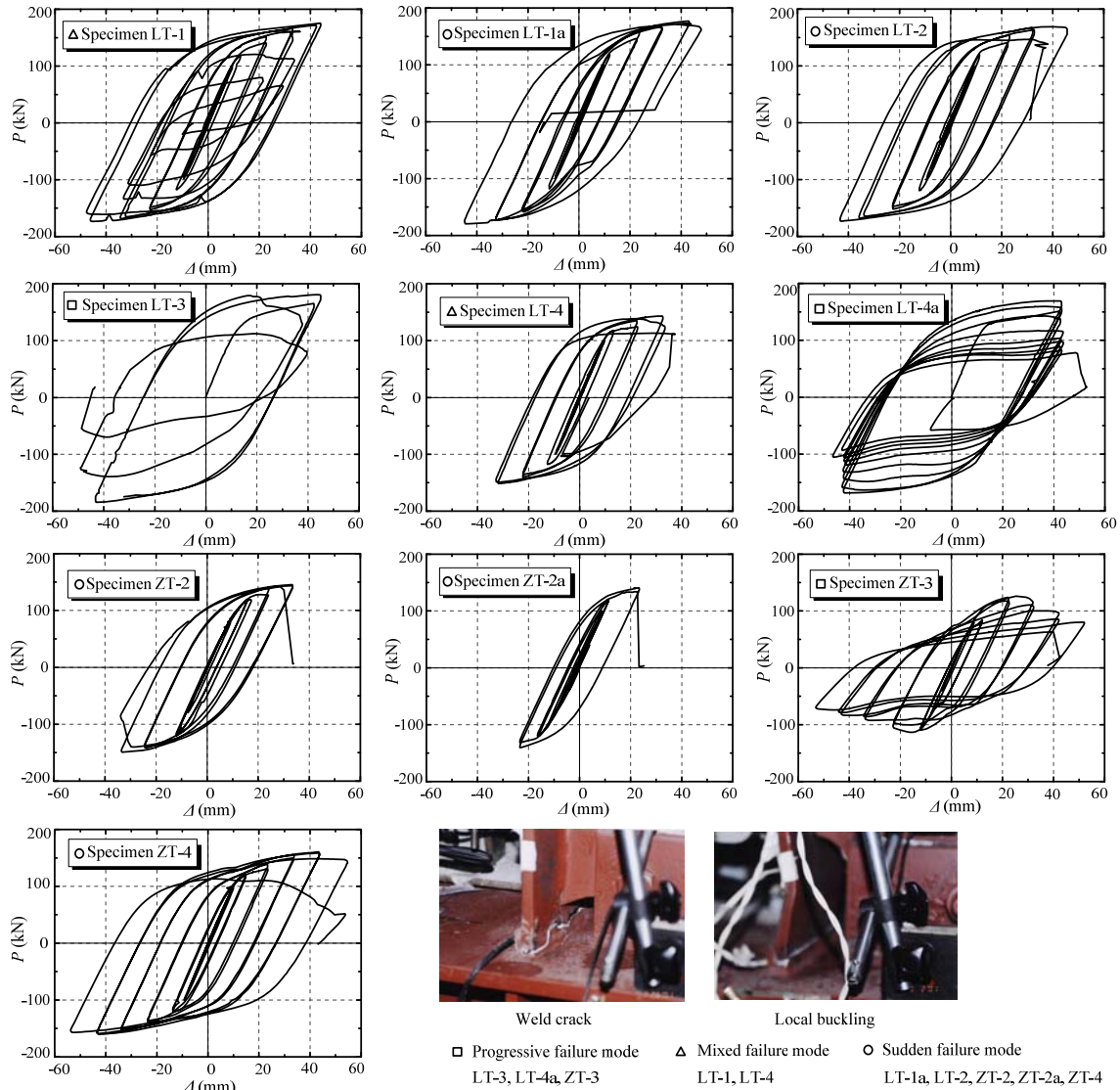


Fig. 6 Hysteretic curves and failure modes of connection specimens

For the specimens LT-1a, ZT-2, ZT-2a, LT-2 and ZT-4, a sudden reduction of strength occurred in last few cycles with limited degradation of strength and stiffness before final failure. This kind of failure had no signs, being called sudden failure mode. Due to lack of lateral restraints, the “Dog bone” specimens ZT-2a, LT-2 fractured at the weld zone and did not formed plastic hinges at the reduced sections (Li *et al.* 2009). The expected ductile failure of such connections did not achieve. Specimens ZT-3, LT-3 and LT-4a underwent progressive degradation of both strength and stiffness as the number of cycles increased, shown as ductile failures with the formation of plastic hinges. The locations of plastic hinges were certain distances away from welds, making the failures occur in base metals not welds. LT-1 and LT-4 firstly exhibited limited strength

degradation, while later specimens were rapidly damaged in last few cycles until failure, indicating mixed failure modes. From all the specimens under different loading patterns, a common phenomenon was found that the sudden failure modes possibly occurred to specimens subjected to stepwise amplitude loadings, while progressive failure modes more possibly occurred to specimens under constant amplitude loadings with large imposed displacements. The probable reasons were as follows: if the first imposed loading displacement was large enough, the plastic hinge would be formed at a certain distance away from the beam root (weld area). The changed failure position caused the change of the failure mode.

2.2 Xiong (2011) tests from Tsinghua University

2.2.1 Specimens description

Nine specimens were tested under various cyclic loading patterns for further study of damage and degradation. The detailed dimensions of beam and column as well as connected method were the same as tests of Chen (2011) as shown in Fig. 2, in which, L_B was 1500 mm for this series. The connection constructions of welded holes were designed according to the recommendation of Chinese standard (shown in Fig. 7). The specimens described in this paper were fabricated from Q345B steel. The material properties of steel were shown in Table 2.

Table 2 Material properties of specimens

Material	Q345 (14 mm)	Q345 (12 mm)	Q345 (8 mm)
Yield strength f_y (MPa)	393.0	359.9	354.5
Ultimate strength f_u (MPa)	547.3	524.7	481.3

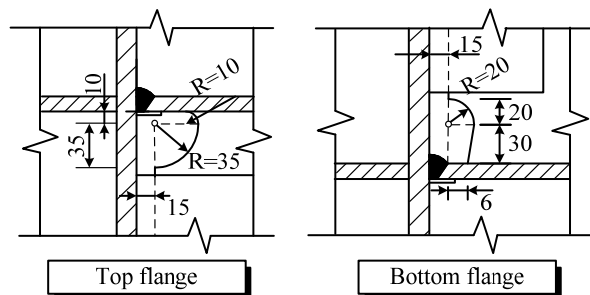


Fig. 7 Constructions of welded holes (mm)



Fig. 8 Experimental equipment

The experiments were conducted using a MTS actuator of ± 5000 kN capacity as shown in Fig. 8. Lateral restraint was applied to prevent global buckling. All the specimens were force-displacement controlled except the specimens under constant amplitude loadings. A series of loading patterns were programmed and summarized in Fig. 9 and Table 3. They simulated various seismic actions of real situations. The combinations of strong and small earthquake waves were adequately considered.

2.2.2 Results and discussion

Table 3 summarized the types of failure, total number of cycles, number of plastic cycles and loading histories. The typical failure modes of the connections were presented in Fig. 10. Hysteretic curves ($P-\Delta$) of specimens were shown in Fig. 11. From the observations, several connections finally fractured at the heat affected zones of top beam flanges (Fig. 10(a)) and the other specimens suffered local buckling (Fig. 10(b)). From the hysteretic curves, it could be clearly

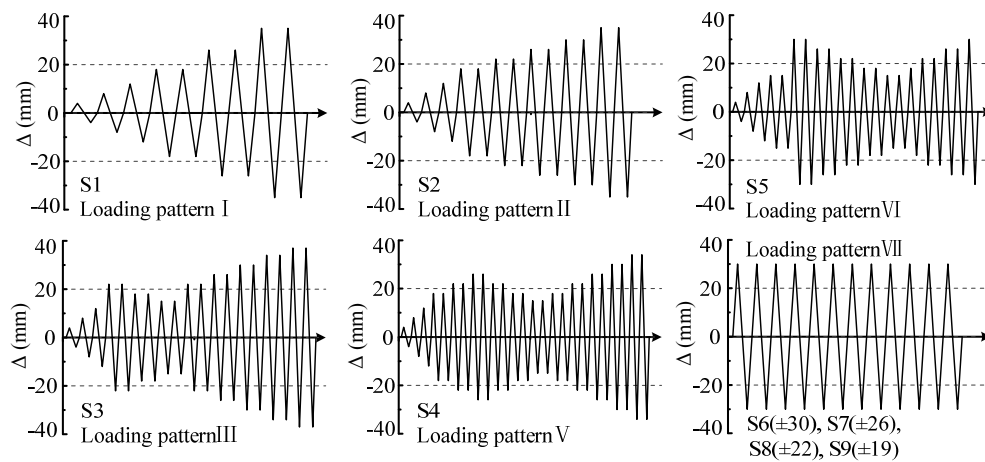


Fig. 9 Cyclic loading patterns

Table 3 Failure parameters of specimens

Spec.	N_{total}	N_p	Loading patterns	Failure modes
S1	12	6	I	○
S2	18	10	II	○
S3	24	16	III	○
S4	34	26	IV	△
S5	25	17	V	△
S6	10	10	VI	□
S7	13	13	VI	△
S8	17	17	VI	□
S9	62	62	VI	□

*Note: □ Progressive failure mode, △ Mixed failure mode, ○ Sudden failure mode

N_{total} = the number of total cycles to failure, N_p = the number of cycles with plastic deformation to failure

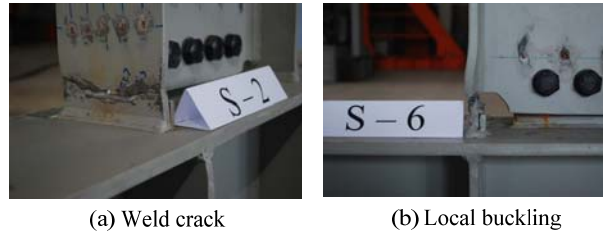


Fig. 10 Typical failure modes

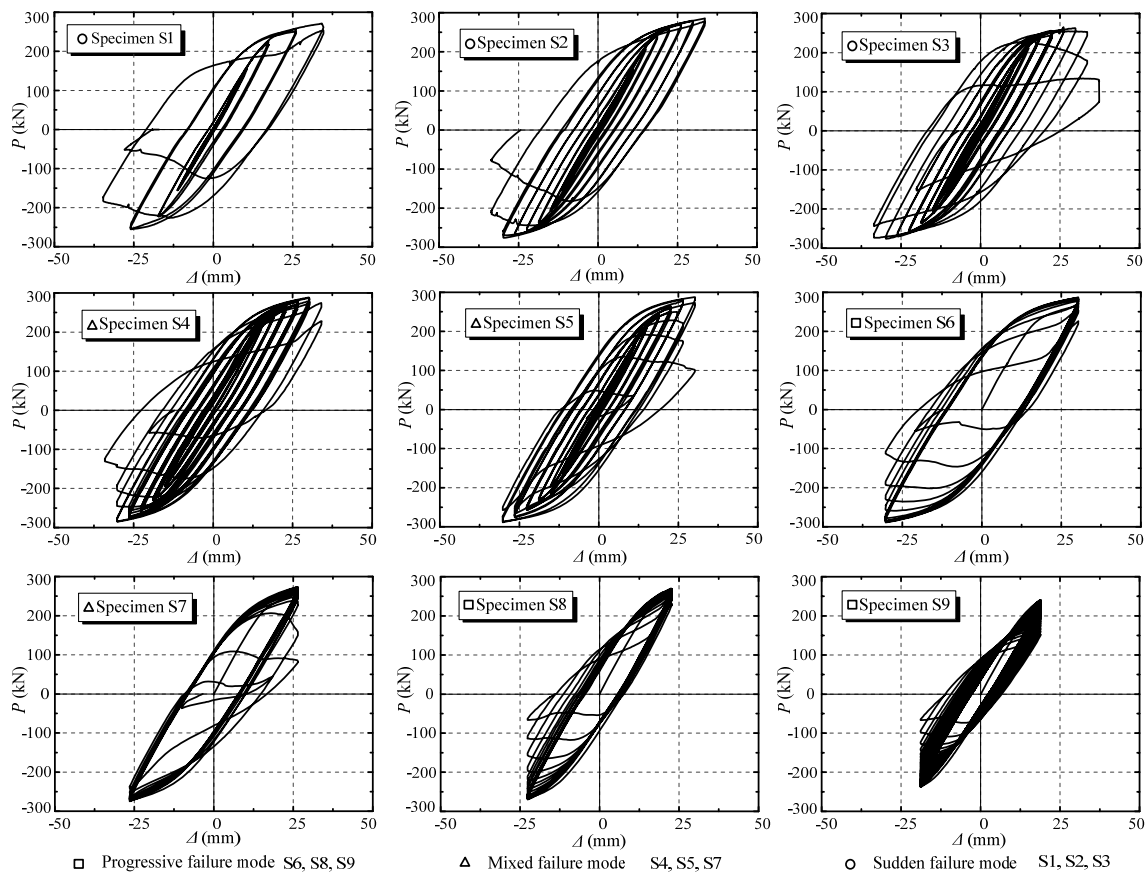


Fig. 11 Hysteretic curves of connection specimens

obtained that loading histories significantly affected the failure modes, indicating that the sequences of ground motions had a significant effect on the responses of steel frame (Loulelis *et al.* 2012). Likewise, specimens under stepwise amplitude loadings were easier to suffer sudden failure modes or mixed failure modes, while the ones under constant amplitude loadings were easier to suffer progressive failure modes, especially under the loading patterns with large displacement amplitudes. The probable reasons were that failure positions were changed subjected to different loading patterns. In addition, the reciprocating loading patterns with small displacements or stepwise amplitudes had less impact on properties of steel base metals than on welds. The welds

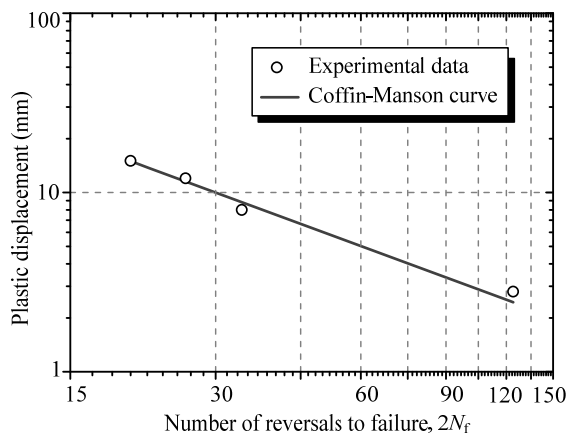


Fig. 12 Coffin-Manson fatigue curve of specimens

would be prone to fatigue failures. By comparing specimens S3~S5, the position of maximum imposed displacement in loading pattern affected the position of carrying capacity in experimental curve, but had little effect on final failure modes. Based on test results, a sudden reduction of strength occurred (brittle failure mode) for specimens S1~S3 in final cycles with limited degradation during the previous cycles. Specimens S6 and S8~S9 underwent progressive degradation of strength and stiffness as the number of cycles increased, which presented ductile failures with forming plastic hinges. Specimens S4~S5 and S7 firstly exhibited the progressive degradation, and then were destroyed suddenly, that meant the specimens suffered mixed failure modes. Though S7 was subjected to constant amplitude loading with relatively large displacement, it still underwent mixed failure due to worse welded quality.

For specimens under constant amplitude loadings (S6~S9) in this study, the failures presented the low-cycle fatigue characteristics. Plastic displacement-cycles data from tests approximately fell on a straight line when they were plotted on a log-log scale graph. This observation was Coffin-Manson relationship (Manson 1953, Coffin 1954), shown as below;

$$\frac{\Delta\delta_p}{2} = \delta'_f (2N_f)^c \quad (1)$$

Where, $\Delta\delta_p$ is the plastic displacement amplitude, δ'_f is the fatigue ductility coefficient, parameter c is the fatigue ductility exponent, and $2N_f$ is the number of reversals to failure.

In order to calibrate material parameters of Coffin-Manson relationship (Eq. (1)), the total displacement amplitudes were resolved into elastic components and plastic components. The plastic displacements and cycle numbers of S6~S9 specimens were adopted for data fitting. Fig. 12 showed a satisfactory fitting result, and then fatigue parameters were obtained, which were $\delta'_f = 318$ and $c = -1.02$ (correlation coefficient R was 0.985).

3. Comparison among damage index models

The damage process inevitably changed the redistribution of internal forces of members, affecting the final failure modes significantly. Damage index D is always used for damage

prediction. Therefore, it is necessary to discuss the accuracy and applicability of damage index models. Based on above mentioned experimental data, the comparison among different damage index models was carried out.

3.1 Damage index models

Damage index D has the following characteristics: (1) the range of damage index is within $[0, 1]$. When $D = 0$, the structure is non-damaged; and when $D = 1$, the structure is completely destroyed. When $0 < D < 1$, the structure is damaged in varying degrees. (2) Damage index D is a monotonously increasing function, indicating that damage process is irreversible (Li *et al.* 2004).

The influencing factors of damage index models are quite complicated. They are commonly expressed by cumulative variables, e.g., plastic strain, plastic strain energy, plastic displacement, and plastic dissipative energy. The structural engineers are commonly interested in the global behaviors of structures rather than local ones. Hence, for life assessment of a structure, it is convenient to describe the degradation and damage behaviors of stiffness and strength with global variables (Castiglioni and Pucinotti 2009). In this paper, macro parameters (imposed forces and imposed displacements) were adopted for damage index models instead of micro parameters such as stresses and strains.

The proposed models in References can be summarized into three categories in terms of independent variables: (1) damage index models based on dissipative energy, (2) damage index models based on plastic displacement, (3) damage index models based on both dissipative energy and plastic displacement. A brief review of these models was performed in Table 4.

Table 4 Summary of damage index models

Categories	Damage index models	Description
	(1) Darwin model $D_D = \sum_{i=1}^N \frac{E_i}{F_y \cdot (S_u - S_y)}$	Darwin and Nmai (1985) considered each structure or member had a certain amount of plastic energy dissipation capacity. The failure occurred when the plastic energy had been exhausted.
Dissipative plastic energy	(2) Gosain model $D_G = \sum_{i=1}^N (\mu_{st} - 1) \lambda_i$	Gosain <i>et al.</i> (1977) proposed a cumulative energy model by multiplying plastic deformations and forces.
	(3) Ibarra model $D_I = \left(\frac{E_i}{E_t - \sum_{j=1}^i E_j} \right)^c$ <p>$1 \leq a \leq 2$ was defined.</p>	Ibarra <i>et al.</i> (2005) improved the model of Rahnama <i>et al.</i> (1993). The model indicated the damage value at cycle i was the ratio of dissipated energy of i th cycle and remainder energy.
Plastic displacement	(4) Krawinkler model $D_K = \sum_{i=1}^N (\mu_{st} - 1)^b$ <p>$1 \leq b \leq 2$, in which, b was proposed as 1.8 for steel structures.</p>	Krawinkler and Zohrei (1983) suggested that the degradation cumulated according to cumulative plastic deformation. Different cycles of plastic deformation played various weights.

Table 4 Continued

Plastic displacement	<p>(5) Dong model</p> $D_{DB} = (1 - \eta) \frac{S_{i,\max} - S_y}{S_u - S_y} + \eta \cdot \sum_{i=1}^N \frac{S_i - S_y}{S_u - S_y}$ <p>η was suggested as 0.0081.</p>	<p>Sometimes, the peak displacement of seismic had great effect on structures. Therefore, the model of Dong and Shen (1997) emphasized the importance of the cycle with maximum plastic deformation. The weight of this cycle was adequately considered.</p>
	<p>(6) Newmark model</p> $D_N = \sum_{i=1}^N (\mu_{si,\max} - 1)$	<p>The model of Newmark mentioned in Castiglioni and Pucinotti (2009) was described as the maximum ratio of imposed plastic displacement per cycle and yield displacement of structure.</p>
Energy and plastic displacement	<p>(7) Park model</p> $D_P = \left[\max(\mu_{st}) + \omega \cdot \sum_{i=1}^N \alpha_i \right]$ <p>ω was proposed as 0.025 for steel structure.</p>	<p>The model of Park and Ang (1985) was firstly used in concrete structures, considering both the maximum plastic deformation and plastic dissipated energy. The model enhanced the effect of maximum imposed displacement.</p>
	<p>(8) Banon model</p> $D_B = \sqrt{(\mu_{si,\max} - 1)^2 + \left(\sum_{i=1}^N h \cdot (2 \cdot \alpha_i)^d \right)^2}$ <p>The values of $h = 1.1$ and $d = 0.38$ were adopted for parameters.</p>	<p>The model of Banon <i>et al.</i> (1981) combined the maximum plastic deformation and plastic dissipated energy based on a non-linear function. The weights of the cycles with maximum deformations were also emphasized.</p>
	<p>(9) Ou model</p> $D_{OU} = \left(\frac{S_{si,\max}}{S_u} \right)^\beta + \left(\frac{\sum_{i=1}^N E_i}{E_u} \right)^\beta$ <p>β was commonly defined as 2 in case of steel structure.</p>	<p>In the model of Ou <i>et al.</i> (1990), maximum plastic deformation and cumulative plastic dissipated energy were both considered based on an exponential function.</p>
	<p>(10) Hwang model</p> $D_H = \sum_{i=1}^N (\mu_{st} - 1)^\varphi \cdot \lambda_i^\gamma \cdot \alpha_i^\zeta$ <p>The constant parameters $\varphi = \gamma = \zeta = 1$ were adopted.</p>	<p>Hwang and Scribner (1984) model mixed all the reported factors, including the ratios of imposed plastic displacement, reaction force and dissipated energy. The weight of each variable was controlled by exponent parameters.</p>

* Note: the mentioned damage parameters above were defined in **Notation** list

3.2 Damage index models comparison

According to the definition of damage index, the parameters of various models were calibrated against experimental data by defining the value of damage index attaining 1.0 in failure cycle. Figs. 13 and 14 showed the applied comparisons of various damage index models on tests. The damage

developing curves described by various models for connections were analyzed and discussed. Furthermore, the predictive ability and applicability for actual cyclic behaviors of typical steel connections were compared.

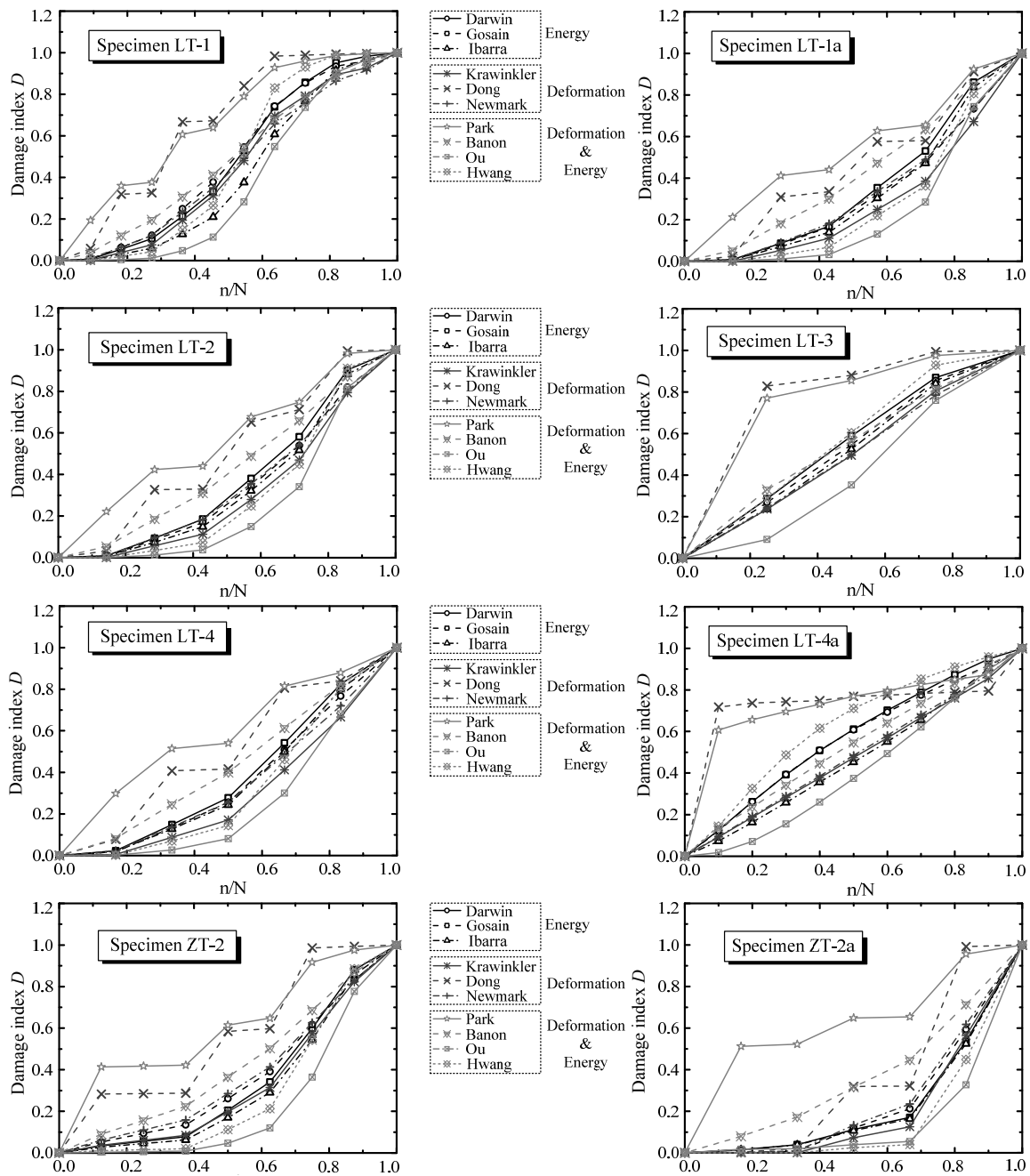


Fig. 13 Comparison of damage indices for experimental specimens (Chen (2001) series)

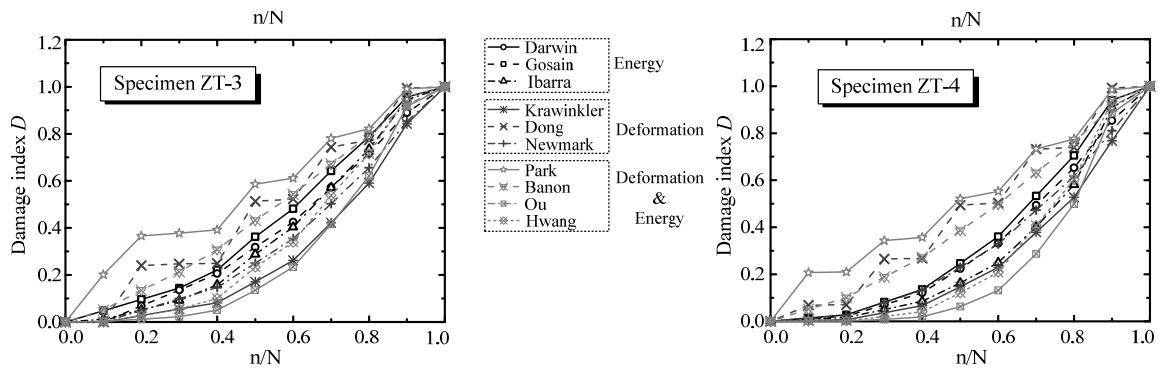


Fig. 13 Continued

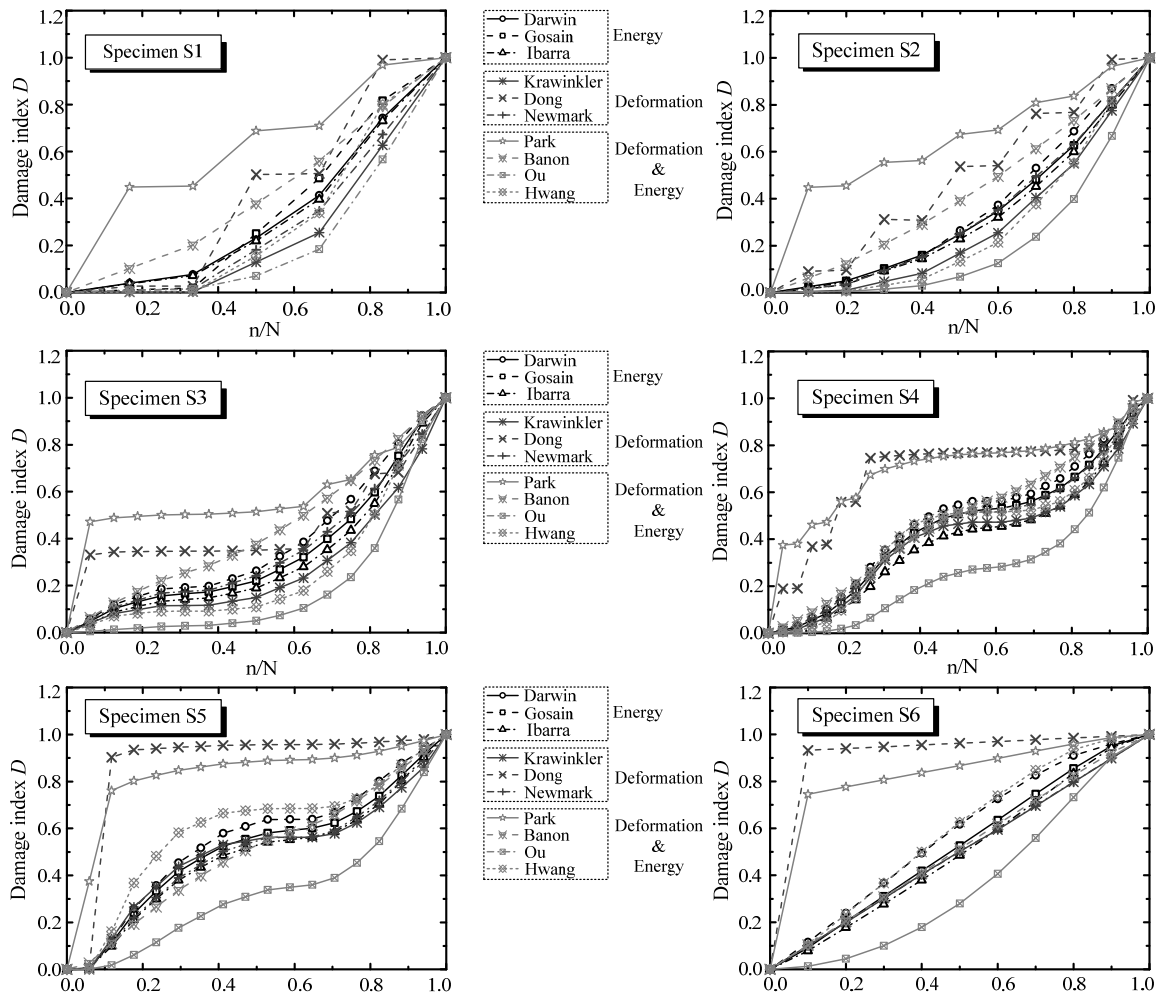


Fig. 14 Comparison of damage indices for experimental specimens (Xiong (2011) series)

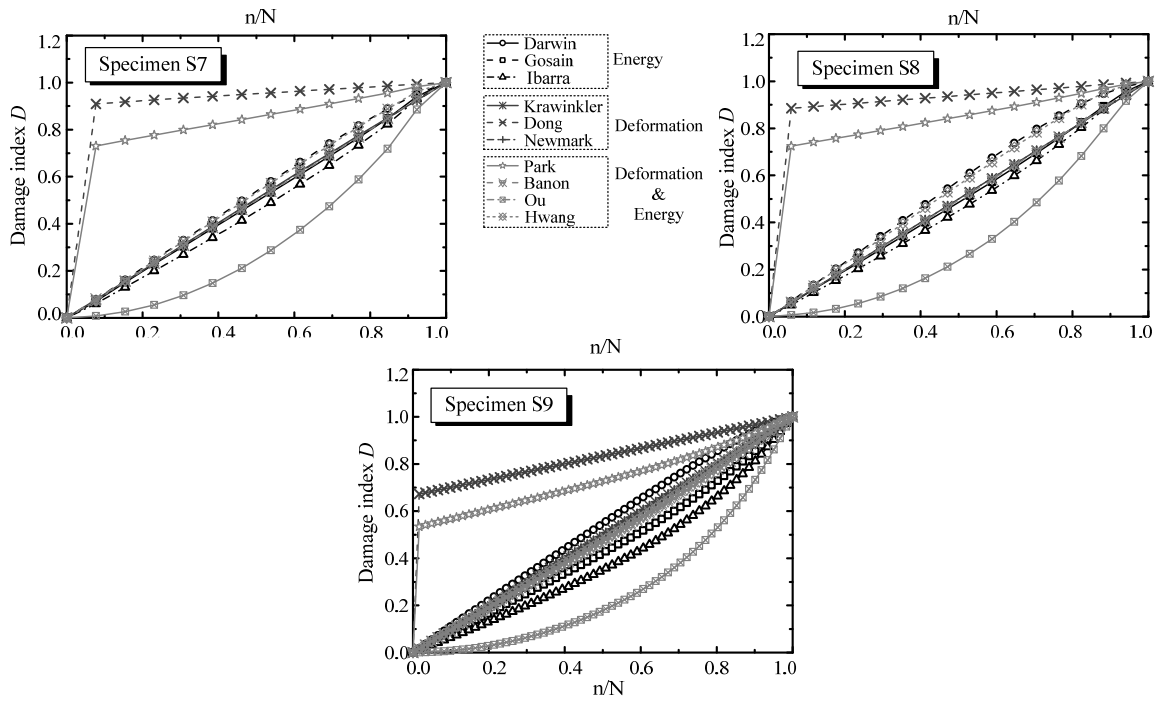


Fig. 14 Continued

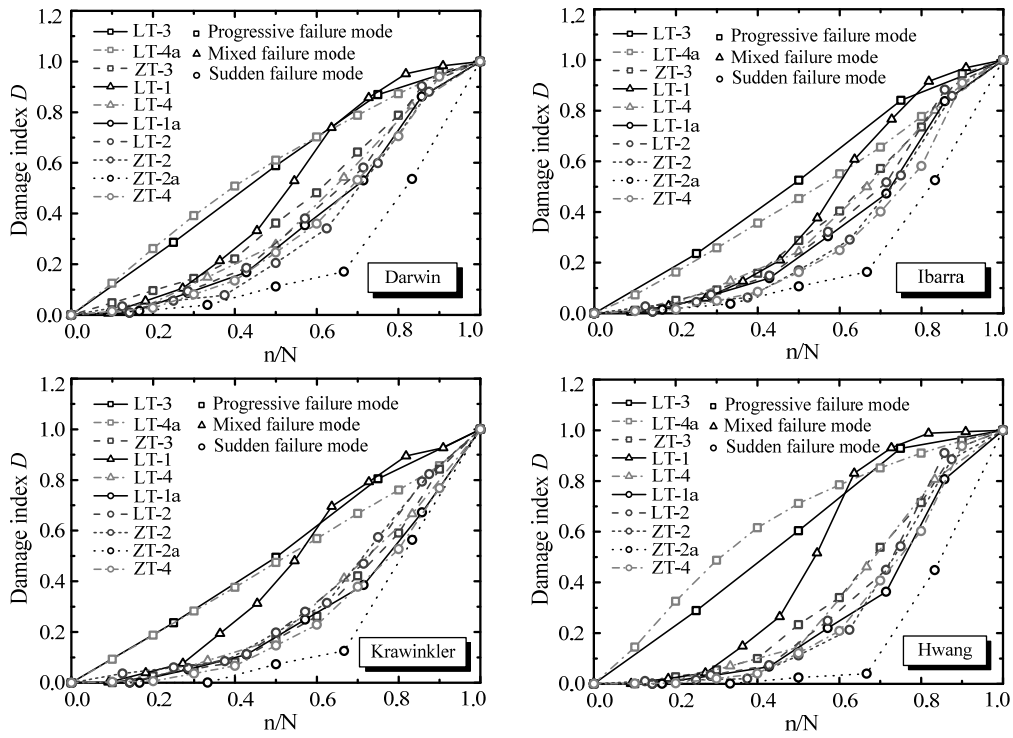


Fig. 15 Application of four damage index models

Darwin, Gosain and Ibarra damage index models took into account the dissipative energy. The distributive curves of three models were similar and located at the intermediate position of all predicted curves. The curves of Ibarra model presented a little lower than the other two index models with energy variable. Among these three models, the damage curves of Darwin model was in best accordance with each type of failure mode. The values of damage index calculated by these three models increased with the increment of plastic cycles, due to the increasing hysteretic area of each cycle.

Krawinkler and Newmark damage index models were based on plastic deformations. The curves of Krawinkler model presented an exponent relationship with plastic displacements while the curves of Newmark model were linearly correlative with plastic displacements. Therefore, the damage rate of Krawinkler index model slowed down during the stage with smaller imposed displacements. For constant amplitude loading patterns, the damage curves of both models were linear, because displacements as the unique variable were invariable.

Dong damage index model contained two parts: one part was caused by the cycle of history maximum displacement and the other part was caused by other cycles. The contribution of peak displacement during loading process was adequately considered. In terms of this feature, the curves presented obvious rough and ladder-like characteristic (the value of damage index nearly remained unchanged under the same displacement loading). The phenomenon indicated that the cumulative effect was not obvious under the same displacement loading. The influence of this ratio $S_{i,\max} - S_y / S_u - S_y$ increased as the cycle's amplitude increased. In the case of stepwise increasing amplitude loadings, the damage curves were relatively smoother. For constant amplitude loadings, the first plastic cycle significantly affected the predicted curves of damage. The values of the damage index were within 0.50 and 0.80.

Park model consisted of both maximum plastic deformation and plastic dissipated energy that comprehensively considered the effects of various variables on structures damage. The distributive shape of curves was ladder-like. This was similar to the curve shape of Dong damage index model, because these two models both enhanced the impact of history maximum displacements on damage curves. Due to the selected value of parameter ω , the influence of cumulative dissipated energy was not remarkable, hence, the degraded degrees were nearly the same without obvious cumulative effect subjected to the same displacement loadings. Likewise, the first cycle amplitude played a great role on damage curves, especially for constant amplitude loadings. The values of damage index could achieve between 0.60 and 0.80 in the first plastic cycle. Therefore, the curves of Dong and Park models were plotted above all the other models in graphs.

Banon model owned the same variables as Park's, including maximum plastic deformation and plastic dissipated energy. However, the model was different from Park model in the proportion of cumulative dissipated energy. Due to the increasing proportion of cumulative dissipated energy, the curves were smoother than Park model's without obvious steps.

The function of Ou model was quadratic and different from Banon and Park models. The damage rate of previous cycles with smaller displacement slowed down. Therefore, the curves of Ou model presented concave and were plotted below all the other models, regardless of constant amplitude loadings or stepwise increasing amplitude loadings. This phenomenon indicated the model could well predict the sudden failure modes.

Hwang model was developed based on Gosain model, consisting of all the cumulative damage variables mentioned previously. The model could predict the failure modes more accurately.

From the point of specimens, LT-1a, LT-2, ZT-2, ZT-2a, LT-4, S1 and S2 were imposed on stepwise increasing amplitude loading patterns. The failure modes of these specimens were sudden

failure with little degradation of strength before last cycle. Except for Park model and Dong model, all the damage index models presented concave curves, which represented the sudden failure. Park model emphasized the effect of first cycle with the selected value of ω , therefore, the curves were different from the ones of other index models.

Specimen S3 suffered sudden failure subjected to “small \rightarrow large \rightarrow small” loading pattern. The curves had obvious inflection points, but were accorded with sudden distributive forms.

LT-3, LT-4a, S6, S8 and S9 underwent progressive degradation of strength and stiffness as the number of cycles increased subjected to constant amplitude loading patterns. Except Ou model, the damage curves of all the other damage index models presented convex or linear forms, representing ductile failure.

Although ZT-3 was imposed on stepwise increasing amplitude loading pattern, the remarkable degradations of strength and stiffness were found during loading process and the damage curves were typically convex.

For mixed failure modes, the damage curves of LT-1 presented typical “S” shape. The curves of LT-4 were closer to the forms of sudden failure mode. S4 and S5 suffered variously changing amplitude loadings, whose curves presented multi-wave shapes and the curves were between the sudden failure curves and progressive failure curves. Although specimen S7 was imposed on constant amplitude loading, the failure mode was also mixed failure. Most of damage index models could not provide good predictions for this situation.

From analysis results, loading histories significantly affected the distributive shapes of the damage index models. The models with only displacement variable seriously relied on loading histories. Furthermore, the selected parameters of damage index models affected the developing trends of curves. In fact, they should be obtained according to the specimens' own characteristics. However, the parameters of existing models were constant values and were independent on specimen properties. For the damage index models considering both maximum plastic deformation and plastic dissipated energy, the selected parameters would influence the predicted results. For example, comparing the damage curves of Park model and Banon model, the proportions of two variables significantly affected the distributions of curves.

In a word, different models had different distributive descriptions for the same structure, which indicated the damage index models had their own scopes of application. For example, Park model and Dong model were more applicable for the prediction of progressive failure and Ou model was more suitable for the prediction of sudden failure.

3.3 Application of four damage index models

For the models with different variables, the index models of Darwin, Ibarra, Krawinkler and Hwang gave relatively better predictions for failure modes (progressive, sudden or mixed failure modes). Fig. 15 presented the applications of these four damage index models for two series specimens. The curves of Hwang model were in best accordance with the criteria reported by Castiglioni *et al.* (2009). Darwin and Ibarra models with energy variable could also well describe the damage developing trends. However, the expressions of these models were a little complicated. When they were embedded and implemented into software, continuous integration of per cycle was needed for calculating hysteretic energy, which remarkably reduced the computational efficiency. The expression of Krawinkler model was the simplest with only displacement variable. The model only needed to record the current variables, which was convenient to achieve in program.

4. Conclusions

Base on two series of beam-to-column tests subject to cyclic quasi-static loading patterns, the degradation and damage behaviors were analyzed and discussed. The important parameters of cumulative variables were calculated, including dissipative energy, cumulative energy, loading displacement, imposed force, yield displacement, and yield force of each connection. In terms of these calculative data, the comparison and application of ten damage index models were carried out for failure prediction. The damage curves of specimens were obtained based on various damage index models. According to the experimental results and data analysis, the following conclusions can be drawn.

1. The loading history significantly affected the failure modes and distributive shapes of damage index models. Specimens under stepwise amplitude loadings were easier to sudden failure modes or mixed failure modes, while the ones under constant amplitude loadings were easier to progressive failure modes, especially with large displacement amplitudes. The probable reasons were that the failure positions were changed subjected to different loading patterns. In addition, the reciprocating imposed loadings with small displacements or stepwise amplitudes had smaller impact on properties of steel base metal, while had significant impact on welds, and the welds would be prone to fatigue failures. The models with only displacement variable seriously relied on loading histories.
2. Different models had different distributive descriptions for the same structure, indicating that the damage index models had their own scope of application. For the index models considering both maximum plastic deformation and plastic dissipated energy, the selected parameters would influence the predicted results. Comparing the damage curves of Park model and Banon model, the proportions of the two variables significantly affected the distribution of curves.
3. The selected parameters of the damage index models affected the distribution of damage curves. In fact, they should be determined based on their own characteristics of specimens. However, the parameters of existing models were constant values and were independent on specimen properties.
4. Although the multi-variable index models were in better accordance with the failure criterions reported by references, the expressions of these models were a little complicated. When they were implemented into software, integration of per cycle was needed for calculating hysteretic energy, which remarkably reduced the computational efficiency. The expression of Krawinkler model was simplest with only displacement variable. It only needed to record the current results and was convenient to achieve in program.

Acknowledgements

This work was supported by the National Natural Science Foundation (No. 51038006).

References

- Ballio, G., Calado, L. and Castiglioni, C.A. (1997), "Low cycle fatigue behaviour of structural steel members and connections", *Fatigue Fract. Eng. Mater. Struct.*, **20**(8), 1129-1146.
- Banon, H., Biggs, J. and Irvine, H. (1981), "Seismic damage in reinforced concrete frames", *J. Struct. Eng.*,

- 107(9), 1713-1728.
- Castiglioni, C.A., Mouzakis, H. and Carydis, P. (2007), "Constant and variable amplitude cyclic behavior of welded steel beam-to-column connections", *J. Earthq. Eng.*, **11**(6), 876-902.
- Castiglioni, C.A. and Pucinotti, R. (2009), "Failure criteria and cumulative damage models for steel components under cyclic loading", *J. Construct. Steel Res.*, **65**(4), 751-765.
- Chen, H. (2001), "Seismic brittle fracture mechanism and seismic behavior of steel beam-column connections in tall building", Doctoral Dissertation, Xuzhou: *China University of Mining and Technology*, 25-85.
- Coffin, L.F. (1954), "A study of the effects of cyclic thermal stresses on a ductile metal", *Transact. ASME*, 76.
- Darwin, D. and Nmai, C.K. (1986), "Energy dissipation in RC. beams under cyclic load", *J. Struct. Eng.*, **112**(8), 1829-1846.
- Dong, B. and Shen, Z.Y. (1997), "An experiment-based cumulative damage mechanics model of steel under cyclic loading", *Adv. Struct. Eng.*, **1**(1), 79-87.
- Egor, P., Yang, T. and Chang, S. (1998), "Design of Steel MRF Connections before and after 1994 Northridge Earthquake", *Eng. Struct.*, **20**(12), 1030-1038.
- Gosain, N.K., Brown, R.H. and Jirsa, J.O. (1977), "Shear requirement for load reversals on RC members", *J. Struct. Eng.*, **103**(7), 1461-1476.
- Hwang, T.H. and Scribner, C.F. (1984), "R/C member cyclic responses during various loadings", *J. Struct. Eng.*, **110**(3), 477-489.
- Ibarra, L.F. and Krawinkler, H. (2005), "Global Collapse of Frame Structures under Seismic Excitations", *Pacific Earthquake Engineering Research Center*, Report 06.
- Ibarra, L.F., Medina, R.A. and Krawinkler H. (2005), "Hysteretic models that incorporate strength and stiffness deterioration", *Earthq. Eng. Struct. Dyn.*, **34**(12), 1489-1511.
- Krawinkler, H. and Zohrei, M. (1983), "Cumulative damage in steel structures subjected to earthquake ground motion", *Comput. Struct.*, **16**(1-4), 531-541.
- Li, F.X., Kanao I., Li, J. and Morisako, K. (2009), "Local Buckling of RBS Beams Subjected to Cyclic Loading", *J. Struct. Eng.*, **135**(12), 1491-1498.
- Li, H.Q., Zuo, Q.G., Yu, Z.C., Jiang, Y.Q. and Xilin, L.V. (2004), "Analysis and experiment of cumulated damage of steel frame structures under earthquake action", *J. Build. Struct.*, **25**(3), 69-74.
- Li, J. (2002), "Investigation on energy dissipation and accumulative damage of welded beam-to-column connections under earthquake cyclic loading", Ph.D. Dissertation, College of Materials Science & Engineering, Tianjin University, Tianjin, China.
- Lignos, D. (2008), "Sidesway collapse of deteriorating structural system under seismic eExcitations", Ph.D. Dissertation, Department of Civil and Environmental Engineering, Stanford University, Stanford, CA.
- Loulelis, D., Hatzigeorgiou, G.D. and Beskos, D.E. (2012), "Moment resisting steel frames under repeated earthquake", *Earthq. Struct. Int. J.*, **3**(3), 231-248.
- Manson, S.S. (1953), "Behavior of materials under conditions of thermal stress, heat transfer symposium", University of Michigan Engineering Research Institute.
- Ministry of Housing and Urban-Rural Development of the People's Republic of China (2001), *GB50011-2001 Code for Seismic Design of Buildings*, China Architecture & Building Press, Beijing, China.
- National Natural Science Foundation Committee (2006), *Subject Development Strategy Research Report-Construction*, Environment and Civil Engineering II, Beijing, Science Press.
- Ou, J.P., Niu, D.T. and Wang, G.Y. (1990), "Fuzzy dynamical reliability analysis and design of muti-storey nonlinear a seismic steel structures", *Earthq. Eng. And Eng. Vib.*, **10**(4), 27-37.
- Park, Y.J., Ang, A.H.S. (1985), "Mechanistic seismic damage model for reinforced concrete", *J. Struct. Eng.*, **111**(4), 722-39.
- Papagiannopoulos, G.A. and Beskos, D.E. (2011), "Modal strength reduction factors for seismic design of plane steel frames", *Earthq. Struct. Int. J.*, **2**(1), 65-88.
- Rahnama, M. and Krawinkler, H. (1993), "Effect of soft soils and hysteresis models on seismic design

- spectra”, Blume Earthquake Engineering Research Center, Report No. 108, Department of Civil Engineering, Stanford University, Stanford, CA, USA.
- Xiong, J. (2011), “Research on the damage behavior and calculation model of welded connections in steel frames under earthquakes”, Doctoral Dissertation, Tsinghua University, Beijing, China.
- Wang, M., Shi, Y.J. and Shi G. (2009(S)), “Analysis on degraded and damage hysteretic model of high-rise steel frame structures and connections”, *Industrial Construction*, 973-981.
- Zareian, F. (2006), *Simplified Performance-Based Earthquake Engineering*, Department of Civil and Environmental Engineering, Stanford University, Stanford, CA, USA.

CC

Notation

The following symbols are used in this paper:

N_{total}	=	<i>the number of total cycles to failure</i>
N_p	=	<i>the number of cycles with plastic deformation to failure</i>
L_B	=	<i>the beam length of connection</i>
P	=	<i>the reaction force of beam tip</i>
Δ	=	<i>the displacement of beam tip</i>
$\Delta\delta_p$	=	<i>plastic displacement amplitude</i>
δ'_f	=	<i>the fatigue ductility coefficient (Coffin-Manson model)</i>
c	=	<i>the fatigue ductility exponent (Coffin-Manson model)</i>
$2N_f$	=	<i>the number of reversals to failure</i>
D	=	<i>damage index</i>
E_i	=	<i>plastic dissipated energy at cycle i of structure</i>
F_y	=	<i>the yield force of structure</i>
S_y	=	<i>the yield displacement of structure</i>
S_u	=	<i>the ultimate displacement of structure subjected to monotonic loading</i>
F_i	=	<i>the reaction force of the loading point at cycle i of structure</i>
S_i	=	<i>imposed displacement of the loading point at cycle i of structure</i>
$\lambda_i = \frac{F_i}{F_y}$		
$\mu_{si} = \frac{S_i}{S_y}$		
$\alpha_i = \frac{E_i}{F_y \cdot S_y}$		
$\sum_{j=1}^i E_j$	=	<i>the sum of all the plastic dissipated energy before cycle i</i>
$E_t = \gamma F_y S_y$	=	<i>the total hysteretic energy of structure</i>
γ	=	<i>the capacity parameter of structure plastic energy dissipation</i>
a, b	=	<i>the exponent of degradation rate</i>
$S_{i,\text{max}}$	=	<i>the maximum deformation of structure until cycle i</i>
$\mu_{si,\text{max}}$	=	<i>the maximum μ_{si} of structure until cycle i</i>
E_u	=	<i>the ultimate dissipated energy of structure subjected to monotonic loading</i>
n	=	<i>the number of cumulative cycles until cycle i</i>
N	=	<i>the number of total cycles with plastic deformation to failure</i>